RSC Advances

PAPER

View Article Online
View Journal | View Issue

Cite this: *RSC Adv.*, 2017, **7**, 36208

Surfactant-exfoliated 2D molybdenum disulphide (2D-MoS_2): the role of surfactant upon the hydrogen evolution reaction†

Gabriella B. de-Mello,[ab] Lily Smith,[b] Samuel J. Rowley-Neale,[bc] Jonas Gruber,[a] Simon J. Hutton[cd] and Craig E. Banks *[bc]

Received 5th May 2017
Accepted 20th June 2017

DOI: 10.1039/c7ra05085b

rsc.li/rsc-advances

Surfactant (sodium cholate, SC) mediated liquid (aqueous) phase exfoliation is a common approach to fabricate 2D molybdenum disulphide (2D-MoS_2–SC) nanosheets since it is a facile methodology producing defect free flakes with nanometer lateral sizes. The electrocatalytic behaviour of 2D-MoS_2–SC towards the Hydrogen Evolution Reaction (HER) is benchmarked within acidic media and found to exhibit inferior HER activity to an equivalent mass of pristine 2D-MoS_2 (2D-MoS_2 produced without a surfactant), with HER onset potentials, current densities and Tafel values of −0.61 V (*vs.* SCE), −2.19 mA cm^{-2}, 141 mV dec^{-1} and −0.42 V (*vs.* SCE), −4.96 mA cm^{-2}, 94 mV dec^{-1} respectively. This work demonstrates that sodium cholate has a detrimental effect upon the HER activity of 2D-MoS_2. Future studies that utilise 2D materials, fabricated *via* liquid surfactant exfoliation, should consider the role of the surfactant in the observed electrochemical responses and perform the necessary control experiments.

Introduction

As a result of the efforts towards mitigating anthropogenic climate change and improving the air quality within heavily urbanised environments, research has intensely focused on finding cost effective less/non-polluting alternatives to the current fossil fuel energy generation methods.[1] A highly promising alternative is hydrogen,[2] produced *via* the electrolysis of water, then, used as a fuel source in fuel cells. However, the requirement of expensive platinum (Pt) as an catalytic electrode material in both electrolysers and fuel cells has severely limited the cost competitiveness of a hydrogen based energy economy.[3]

In order to lower the production costs associated with H_2 (gas), research has recently focused on finding a cheaper more earth abundant electrode material to catalyse the Hydrogen Evolution Reaction (HER) ($2H^+ + 2e^- \rightarrow H_2$),[4] which is the focus of commercially available electrolysers. Studies such as Ji *et al.*[5] have shown that 2D-MoS_2 can be used as an effective electrocatalyst towards the HER. In this case a loading of 48 μg cm^{-2} of 2D-MoS_2 nanosheets onto a glassy carbon (GC) electrode resulted in a low HER over-potential and high current density of −120 mV and 1.26 mA cm^{-2} (η = 150 mV) respectively. The electrochemical properties of 2D-MoS_2 are anisotropic in nature, with the basal plane of the 2D-MoS_2 being relatively inert, whilst the terminated edges of the 2D-MoS_2 will comprise both Mo and S atoms, each having distinct electrocatalytic properties in certain scenarios.[6,7] In this case, it is the dangling bonds of the electronegatively charged S atoms, found at the nanosheet edge sites, which have an affinity for binding electropositive H^+ atoms. This affinity arises from the edge sites having a density functional theory calculated binding energy towards H^+ of +0.08 eV. This strongly implies that the edge S atoms that are responsible for the 2D-MoS_2 nanosheets electrocatalyic activity towards the HER.[6,8,9]

There are numerous methodologies implemented within the literature for the production of 2D-MoS_2 nanosheets; liquid,[10] mechanical,[11] electrochemical (in this case of Bi_2Se_3 and Bi_2Te_3)[12] and shear[13] exfoliation to name just a few. It has also been shown by the work of Li *et al.*[14] that it is possible to fabricate monolayer dichalcogenides by chemical vapor deposition. A common occurrence within these 2D-MoS_2 production techniques, particularly liquid exfoliation, is the incorporation of a surfactant in order to stabilise the 2D materials. Thus, preventing re-aggregation and producing large yields within surfactant–water solutions with relatively defect free flakes with nanometer lateral sizes.[15] For example Howe *et al.*[16] employed a range of bile salts, including: sodium cholate (SC), sodium

[a]*Escola politénica da universidade de São Paulo, Avenida, 380, CEP 05508-900, São Paulo, Brazil*

[b]*Faculty of Science and Engineering, Manchester Metropolitan University, Chester Street, Manchester M1 5GD, UK. E-mail: c.banks@mmu.ac.uk; Web: http://www.craigbanksresearch.com; Fax: +44 (0)1612476831; Tel: +44 (0)1612471196*

[c]*Manchester Fuel Cell Innovation Centre, Manchester Metropolitan University, Chester Street, Manchester M1 5GD, UK*

[d]*Kratos Analytical Limited, Wharfside, Trafford Wharf Road, Manchester, M17 1GP, UK*

† Electronic supplementary information (ESI) available: The characterisation of the 2D-MoS_2 and 2D-MoS_2–SC as well as details of the calculations of the turn over frequency and more a detailed experimental method section is presented. See DOI: 10.1039/c7ra05085b

deoxycholate and sodium taurodeoxycholate in order to stabilise the 2D-MoS_2 dispersion during liquid exfoliation.

Numerous studies within the literature will have employed a surfactant to stabilise various 2D-MoS_2 nanomaterials which has subsequently been explored towards the HER; see Table S1† for a thorough overview. It has been previously noted in an exemplary study by Ambrosi *et al.*,[17] that it is possible to improve the electrochemical HER activity of MoS_2 *via* the addition of organolithium compounds in the exfoliation process. It is also worth noting that the solvent used in the exfoliation process can have a significant effect upon the 2D-MoS_2 activity, with a variation in the HER overpotential from 0.57 to 0.72 V when varying dispersion medias were used (acetonitrile, *N*,*N*-dimethylformamide, ethanol, methanol and water).[18] The work of Guo *et al.*[19] has reported the hydrothermal synthesis of 2D-MoS_2 nanosheets using the surfactant cetyltrimethyl ammonium bromide (CTAB), which was explored towards the HER in acidic media demonstrating a superior response of the CTAB–MoS_2 over that of surfactant free MoS_2. This was attributed to the incorporation of CTAB into MoS_2 sheets inducing better electrical conductivity and exposing additional catalytically-active sites.[19] This likely occurs due to the CTAB preventing the 2D-MoS_2 aggregating back into multi-layer/bulk MoS_2. However, what is evident in this work and those reported within Table S1,† is the question as to whether the observed electrochemical response of 2D-MoS_2 fabricated with a surfactant is solely due to the 2D-MoS_2 or whether the surfactant is contributing, be that detrimental or advantageous, to observed/apparent catalytic properties of the 2D-MoS_2. We note in the work of Guo *et al.*[19] and those reported in Table S1† that control experiments, that is, just a surfactant modified electrode/surface explored towards the HER are lacking.

In order to explore the effect of a commonly employed surfactant on the HER activity of 2D-MoS_2, we compare and contrast the electrocatalytic activity of 2D-MoS_2 produced using a surfactant, sodium cholate (2D-MoS_2–SC), and pristine 2D-MoS_2 (2D-MoS_2 produced without a surfactant) towards the HER.

Results and discussion

The Experimental section and ESI† detail how the 2D-MoS_2 nanosheets were fabricated from bulk MoS_2 *via* a surfactant mediated liquid phase exfoliation process using the surfactant sodium cholate (SC). This 2D material is denoted as 2D-MoS_2–SC. Independent physicochemical characterisation (see ESI†) reveals the 2D-MoS_2–SC to compromise of nanosheets with average lateral widths and number of layers of *ca.* 120 nm and 2 respectively. TEM images of these 2D-MoS_2–SC nanosheets can be seen in Fig. 1(B). Additionally shown in Fig. 1(A) are commercially purchased surfactant free 2D-MoS_2 nanosheets which have average lateral widths and number of layers *ca.* 62 nm and 3 respectively.[20] XPS, XRD, Raman and extinction spectroscopy further indicate that the 2D-MoS_2–SC and 2D-MoS_2 comprise of high quality/purity nanosheets (see ESI†).

The 2D-MoS_2 and 2D-MoS_2–SC were electrically wired *via* immobilisation upon screen-printed electrodes (SPE; see ESI†

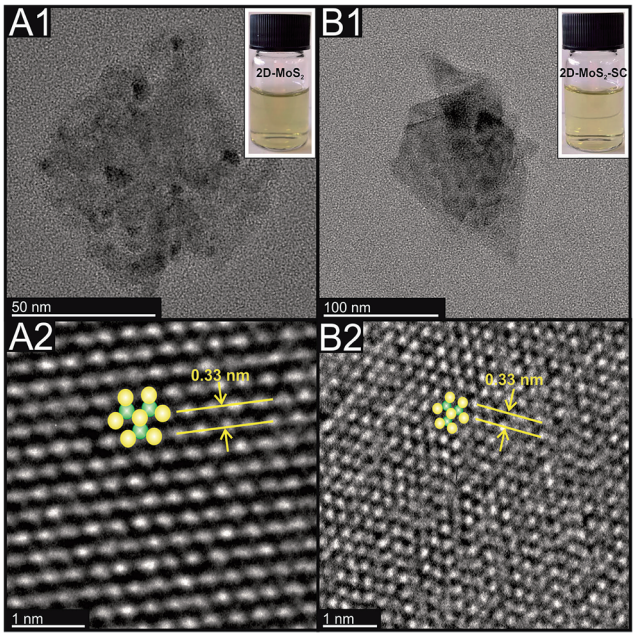

Fig. 1 TEM images of the commercially sourced 2D-MoS_2 (A1) scale bar: 50 nm; (A2) scale bar: 1 nm; and the exfoliated 2D-MoS_2–SC (B1); scale bar: 100 nm, (B2); scale bar: 2 nm.

for details on their fabrication) and explored towards the HER in 0.5 M H_2SO_4, as is common, within the literature.[21] Fig. 2(A) shows typical linear sweep voltammograms (LSV) obtained for a bare/unmodified SPE, SPE modified with *ca.* 2.8 mg cm^{-2} of SC, SPE modified with *ca.* 1725 ng cm^{-2} of 2D-MoS_2, SPE modified with *ca.* 1725 ng cm^{-2} of 2D-MoS_2–SC and a Pt electrode. The bare/unmodified SPE exhibits an HER onset of −880 mV (*vs.* SCE) and a current density of 1.37 mA cm^{-2} at a potential of −1.5 V. The bare SPE exhibits significantly less electrocatalytic activity towards the HER than Pt, which has a HER on set of *ca.* −0.25 V. The observed HER overpotential for Pt is due to it being a metal that has a very small binding energy for H^+.[8] Note that the HER onset is analysed as the potential at which the observed current deviates from the background current by 25 μA cm^{-2}, as is common within the literature.[21]

It is clear upon inspection of Fig. 2(A) that upon electrically wiring 1725 ng cm^{-2} of 2D-MoS_2–SC the HER onset potential becomes less electronegative, shifting by 249 mV to −0.61 V (*vs.* SCE) compared to a bare/unmodified SPE. There is also a corresponding increase in the achievable current to 2.61 mA cm^{-2}. The 2D-MoS_2–SC exhibits a significant benefit towards the HER which arises due to the low binding energy towards H^+ at the edge sites of the 2D-MoS_2–SC nanosheets. From inspection of Fig. 2, the data presented potentially suggests that the 2D-MoS_2–SC is electrocatalytic towards the HER as judged by its improvement over that of a bare SPE. However, if one used pristine 2D-MoS_2 instead the observed result is a much greater HER activity than that of 2D-MoS_2–SC with a HER onset and achievable current of −0.48 V (*vs.* SCE) and 4.29 mA cm^{-2}, respectively. Whilst the 2D-MoS_2 is less electrocatalytic towards the HER than Pt, it is the most beneficial electrocatalyst. We

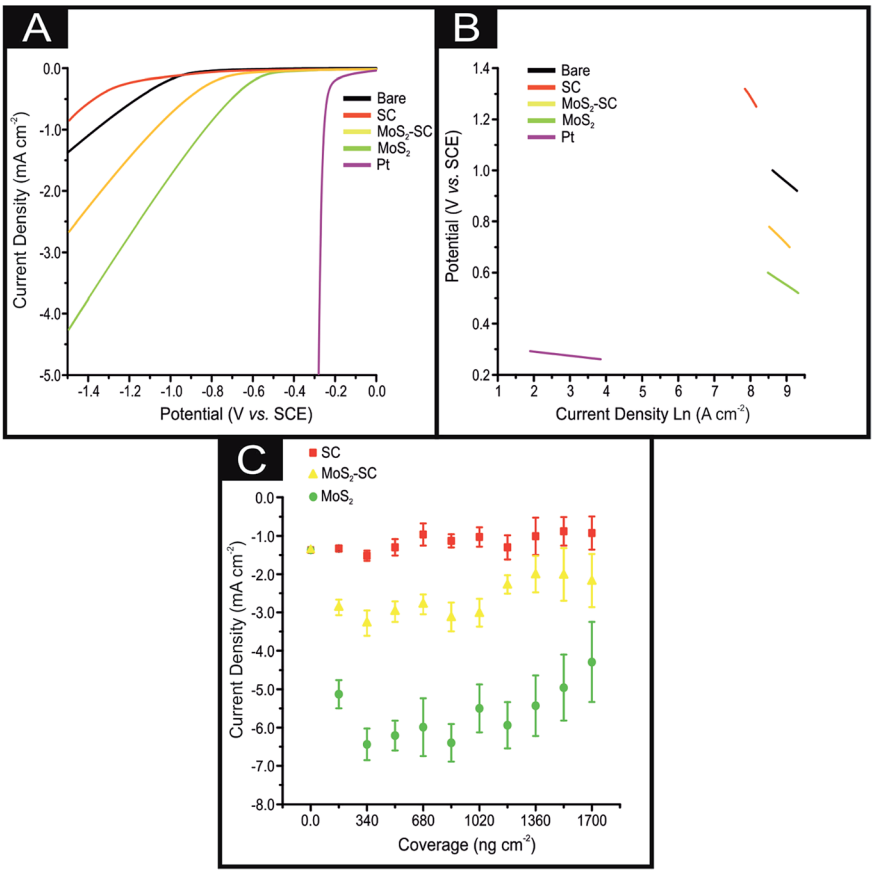

Fig. 2 (A) Linear sweep voltammetry (LSV) of bare/unmodified SPE, SPE modified with *ca.* 2.8 mg cm^{-2} of SC, SPE modified with *ca.* 1725 ng cm^{-2} of 2D-MoS_2, SPE modified with *ca.* 1725 ng cm^{-2} of 2D-MoS_2–SC and a Pt electrode showing the onset of the HER. Scan rate; 250 mV s^{-1} (*vs.* SCE). Solution composition: 0.5 M H_2SO_4. (B) Tafel analysis; potential *vs.* Ln of current density for faradaic section of the LSV presented in (A). (C) The current densities observed at −1.5 V for SPEs modified with 172, 345, 518, 690, 863, 1035, 1207, 1380, 1553 and 1726 ng cm^{-2} of 2D-MoS_2 (green circles) and 2D-MoS_2–SC (yellow triangles) as well as SPEs modified with *ca.* 282, 565, 848, 1131, 1414, 1697, 1980, 2263, 2545, 2828 mg cm^{-2} of SC (red squares) (average standard deviation of 3 replicates). Scan rate; 250 mV s^{-1} (*vs.* SCE). Solution composition: 0.5 M H_2SO_4.

seek to determine why this is the case. Insights from the current literature, for example Guo *et al.*[19] have reported that CTAB–MoS_2 exhibited a superior response towards the HER over that of surfactant free MoS_2 which was attributed to the incorporation of CTAB into MoS_2 increasing the electrical conductivity and exposure of additional catalytically-active sites.[19] However, in our case, we observe the opposite. In order to understand this further, SC (2.8 mg cm^{-2} the equivalent amount of SC present in a solution containing 1725 ng cm^{-2} of 2D-MoS_2–SC) was explored, and as shown within Fig. 2, the HER onset potential is observed to become more electronegative compared to all the nanomaterial and electrodes studied, with the HER observed −1.17 V (*vs.* SCE). There is also a reduction in the achievable current to −0.88 mA cm^{-2} (at a potential of −1.5 V). It is clear that SC, *per se*, has a detrimental effect towards the HER.

Pristine 2D-MoS_2 exhibits an improved HER over the 2D-MoS_2–SC, which is likely due to the presence of the SC blocking/shielding the active edge sites found on the MoS_2 nanosheets resulting in less H^+ being able to freely bind. The pristine 2D-MoS_2 therefore likely has a greater proportion of active edge sites available for H^+ binding than the 2D-MoS_2–SC. As the 2D-MoS_2 demonstrates a greater proficiency at catalysing the HER it may be inferred that the underlying electrochemical reaction mechanism may be different than that of the 2D-MoS_2–SC, SC and bare/unmodified SPE. A common approach within the literature at determining the particular HER mechanism taking place is *via* Tafel analysis on the faradaic regions of the LSV's in Fig. 2(A).[3] For details on how the Tafel slopes displayed in Fig. 2(B) and the Tafel values were determined, interested readers are directed to the ESI.† The Tafel values obtained for the bare/unmodified SPE, SPE modified with 1725 ng cm^{-2} of 2D-MoS_2, 1725 ng cm^{-2} of 2D-MoS_2–SC and 14.14 μg cm^{-2} of SC were found to correspond to 118, 94, 141 and 224 mV dec^{-1}, respectively. Whilst, the Tafel values for the SC and 2D-MoS_2–Sc are too large to be accurately explained by Tafel analysis the obtained values for the bare/unmodified SPE and the modified SPEs suggests poor HER activity with the initial step of H^+ adsorption (Volmer) being the rate limiting step, with a small surface coverage of adsorbed hydrogen.

In order to ascertain the intrinsic catalytic activity being displayed by the 2D-MoS_2 and 2D-MoS_2–SC on a per active site basis. The turn over frequency (ToF) was deduced *via* the methodology presented in the ESI.† The resultant ToF values for

were 0.191 and 0.314 $\frac{H_2/s}{\text{surface site}}$ respectively. These values support the inference that the 2D-MoS_2 is a more beneficial electrocatalyst than the 2D-MoS_2–SC. This could be a result of the SC partially blocking/shielding of the electronegative S atoms located at the active edge sites of the 2D-MoS_2 nanosheets leading to less H^+ adsorption.

Electrochemical HER: critical mass/coverage of 2D-MoS_2 modification

Next, we investigated whether the greater electrocatalytic activity displayed by the 2D-MoS_2 over the 2D-MoS_2–SC is observed across a range of different coverages/masses of modification. The electrochemical response was monitored as a function of coverage: 172, 345, 518, 690, 863, 1035, 1207, 1380, 1553 and 1726 ng cm^{-2} of 2D-MoS_2 and 2D-MoS_2–SC, as well as SPEs modified with *ca.* 282, 565, 848, 1131, 1414, 1697, 1980, 2263, 2545, 2828 mg cm^{-2} of SC (the equivalent amount of SC present in a solution containing 2D-MoS_2–SC). These results are displayed within Fig. 2(C) that show that the 2D-MoS_2 has a greater achievable current (current density recorded at −1.5 V) across the full range of coverages than the 2D-MoS_2–SC. The SC displays no catalytic activity at any coverage, in fact, it results in a decrease in the achievable current. It is evident through inspection of Fig. 2(C) that a trend of increased current density (corresponding to increased 2D-MoS_2 nanosheet coverage (ng cm^{-2})) is subsequently followed by a decrease in current density and/or plateauing effect. This is apparent upon modification of both sets of SPEs modified with 2D-MoS_2 and 2D-MoS_2–SC. A previous study by Rowley-Neale *et al.*[3] observed a similar trend and employed the term "critical mass" for the mass of modification where HER activity is no longer correlated to increased MoS_2 nanosheet deposition. Rowley-Neale and co-workers suggest that a critical mass of modification arises due to instability of the 2D-MoS_2 nanosheets causing delamination from the platforms surface and/or a optimal ratio of active edge sites to inert basal planes being achieved after which subsequent mass additions cause shielding of the edge sites and a detrimental decrease in this ratio. The results of the above study strongly support the aforementioned inference that SC has a detrimental effect upon the ability of 2D-MoS_2 nanosheets to catalyse the HER when used a surfactant in the nanosheets production. The detrimental effect upon the HER activity of 2D-MoS_2–SC might be due to the presence of the SC blocking/shielding the active edge sites found on the 2D-MoS_2 nanosheets resulting in less H^+ being able to freely bind.

Comparing our results to the current literature, as overviewed in Table S1,† we find control experiments, that is, just exploring the response of the surfactant towards the HER is seldom performed. For example Zhang *et al.*[22] compared 3D MoS_2–poly(-vinylpyrrolidone) nanospheres against surfactant free 2D-MoS_2 nanosheets. However, they do not implement any control measurements but problematically are comparing different materials (3D-MoS_2 *vs.* 2D-MoS_2). In the case of the 2D-MoS_2–CTAB reported by Guo *et al.*[19] whilst similar 2D-materials are compared, the control experiment of just the CTAB is critically missing. It is likely in both these cases the surfactant contributes towards the HER activity, that is, itself and potentially producing a favourable orientation to expose active edge sites, albeit they utilise a different surfactant, however one cannot judge or determine the true origin of the response of the MoS_2 material towards the HER this without the proper controls.

The above study, by highlighting the detrimental effect that SC has upon the signal output (HER activity) of 2D-MoS_2 nanosheets, emphasizes the necessity of future studies to perform thorough control experiments in order to ascertain the effect (if any) that a surfactant is having upon the signal/electrochemical output of a particular 2D-material.

Experimental section

All chemicals used were of analytical grade and were used as received from Sigma-Aldrich without any further purification, this includes the bulk MoS_2 powder that was utilised in the fabrication of surfactant exfoliated 2D-MoS_2 (2D-MoS_2–SC).[23] The bulk MoS_2 powder has a reported lateral width of *ca.* 90 nm and a reported purity of 99% (trace metal basis).

The methodology for producing the 2D-MoS_2–SC is a modification of the methods reported previously by Kurapati *et al.*[24], Coleman *et al.*[25], and Smith *et al.*;[15] bulk MoS_2 was procured from Sigma Aldrich (see above), after which it was sonicated in an aqueous solution (water, pH 7.6) containing sodium cholate to induce liquid phase exfoliation. For a full description of the surfactant based liquid exfoliation, sonication and centrifugation methodology utilised herein to produce the 2D-MoS_2–SC, see the ESI.† The surfactant free (pristine) 2D-MoS_2 nanosheets were commercially sourced and have a reported purity of >99% and are dispersed in ethanol at a concentration of 18 mg L^{-1}.[20] The suspended flakes are reported to have an average lateral flake size of 100–400 nm and a thickness of between 1 and 8 monolayers and had not been oxidised, reduced or chemically modified in anyway.[20]

A full independent physicochemical characterisation was performed on the commercially sourced 2D-MoS_2 and the 2D-MoS_2–SC. This included TEM, XPS, Raman spectroscopy and XRD the results of which are detailed within the ESI.† Both the 2D-MoS_2 and the 2D-MoS_2–SC were revealed to comprise of high quality 2D-MoS_2 nanosheets for implementation as an electrocatalyst towards the HER.

The lateral length (L_a) and number of layers of both the 2D-MoS_2 and 2D-MoS_2–SC were readily deduced from optical extinction spectroscopy (see Fig. S1(D)†).[13,26,27] A complete methodology of how this technique was performed can be found within the ESI.† From the spectra presented in Fig. S1(D)† the lateral length and number of layers for the 2D-MoS_2 and 2D-MoS_2–SC nanosheets are determined to correspond to 61.5 nm and 3, and 120 nm and 2 respectively. It is important to point out that the lateral size and the number of MoS_2 sheets are for when these are in solution; when immobilised upon a surface these will deviate from these measured values, but is a common issue in all of the literature.

All solutions were prepared with deionised water of resistivity not less than 18.2 MΩ cm and were vigorously degassed prior to electrochemical measurements with high purity, oxygen free

nitrogen. The above ensures the removal of any trace of oxygen from test solutions, which if present would convolute the observed results for HER with the competing oxygen evolution reaction; this is common practice in the literature.[28,29] All measurements were performed in 0.5 M H_2SO_4 and the sulfuric acid solution utilised was of the highest possible grade available from Sigma-Aldrich (99.999%, double distilled for trace metal analysis).

The electrochemical measurements were performed using an Ivium Compactstat™ (Netherlands) potentiostat. Measurements were carried out using a typical three electrode system with a Pt wire counter electrode and a saturated calomel electrode (SCE) reference. The working electrodes were screen-printed graphite electrodes (SPE), which have a 3 mm diameter working electrode. The SPEs were fabricated in-house with the appropriate stencils using a DEK 248 screen-printing machine (DEK, Weymouth, U.K.).[30] These electrodes have been used extensively in previous studies.[3,31–34] The fabrication technique is described within the ESI.† A full description/specification of the equipment utilised in the characterisation of the materials employed is given within the ESI.†

Conclusions

This work has demonstrated that the surfactant used in the liquid exfoliation of 2D-MoS_2 detrimentally effects its electrochemical activity towards the HER; 2D-MoS_2 outperforms 2D-MoS_2–SC with the critical difference being the presence of SC with control experiments elegantly confirming SC is detrimental. Furthermore, a coverage study revealed that the catalytic effect of the 2D-MoS_2 nanosheets increased proportionally with mass deposited until a 'critical mass' (coverage) was achieved, after which the response was observed to plateau/decline. The likely cause of this effect is inferred herein and has clear implications (in this case) when employing other 2D nanosheet materials within the literature.

This study is unique in that we have investigated the effect of a surfactant upon the HER activity of 2D-MoS_2 nanosheets and indicates that future research involving surfactant exfoliated 2D-MoS_2, and indeed other nanomaterials, should consider the electrochemical behaviour of the surfactant utilised.

Conflict of interest

The authors declare no competing financial interest.

Acknowledgements

Funding from the Engineering and Physical Sciences Research Council (Reference: EP/N001877/1), British Council Institutional Grant Link (No. 172726574) is acknowledged. The Manchester Fuel Cell Innovation Centre is funded by the European Regional Development Fund.

References

1 M. G. Schultz, T. Diehl, G. P. Brasseur and W. Zittel, *Science*, 2003, **302**, 624–627.
2 A. Ahmed, A. Q. Al-Amin, A. F. Ambrose and R. Saidur, *Int. J. Hydrogen Energy*, 2016, **41**, 1369–1380.
3 S. J. Rowley-Neale, D. A. C. Brownson, G. C. Smith, D. A. G. Sawtell, P. J. Kelly and C. E. Banks, *Nanoscale*, 2015, **7**, 18152–18168.
4 N. M. Latiff, L. Wang, C. C. Mayorga-Martinez, Z. Sofer, A. C. Fisher and M. Pumera, *Nanoscale*, 2016, **8**, 16752–16760.
5 S. Ji, Z. Yang, C. Zhang, Z. Liu, W. W. Tjiu, I. Y. Phang, Z. Zhang, J. Pan and T. Liu, *Electrochim. Acta*, 2013, **109**, 269–275.
6 G. Li, D. Zhang, Q. Qiao, Y. Yu, D. Peterson, A. Zafar, R. Kumar, S. Curtarolo, F. Hunte, S. Shannon, Y. Zhu, W. Yang and L. Cao, *J. Am. Chem. Soc.*, 2016, **138**, 16632–16638.
7 X. Chia, A. Y. S. Eng, A. Ambrosi, S. M. Tan and M. Pumera, *Chem. Rev.*, 2015, **115**, 11941–11966.
8 B. Hinnemann, P. G. Moses, J. Bonde, K. P. Jørgensen, J. H. Nielsen, S. Horch, I. Chorkendorff and J. K. Nørskov, *J. Am. Chem. Soc.*, 2005, **127**, 5308–5309.
9 R. J. Toh, Z. Sofer, J. Luxa and M. Pumera, *ChemCatChem*, 2017, **9**, 1168–1171.
10 L. Niu, J. N. Coleman, H. Zhang, H. Shin, M. Chhowalla and Z. Zheng, *Small*, 2016, **12**, 272–293.
11 H. Li, J. Wu, Z. Yin and H. Zhang, *Acc. Chem. Res.*, 2014, **47**, 1067–1075.
12 A. Ambrosi, Z. Sofer, J. Luxa and M. Pumera, *ACS Nano*, 2016, **10**, 11442–11448.
13 E. Varrla, C. Backes, K. R. Paton, A. Harvey, Z. Gholamvand, J. McCauley and J. N. Coleman, *Chem. Mater.*, 2015, **27**, 1129–1139.
14 S. Li, S. Wang, D.-M. Tang, W. Zhao, H. Xu, L. Chu, Y. Bando, D. Golberg and G. Eda, *Appl. Mater. Today*, 2015, **1**, 60–66.
15 R. J. Smith, P. J. King, M. Lotya, C. Wirtz, U. Khan, S. De, A. O'Neill, G. S. Duesberg, J. C. Grunlan, G. Moriarty, J. Chen, J. Wang, A. I. Minett, V. Nicolosi and J. N. Coleman, *Adv. Mater.*, 2011, **23**, 3944–3948.
16 R. C. T. Howe, R. I. Woodward, G. Hu, Z. Yang, E. J. R. Kelleher and T. Hasan, *Phys. Status Solidi B*, 2016, **253**, 911–917.
17 A. Ambrosi, Z. Sofer and M. Pumera, *Small*, 2015, **11**, 605–612.
18 X. J. Chua and M. Pumera, *Phys. Chem. Chem. Phys.*, 2017, **19**, 6610–6619.
19 Z. Guo, Q. Ma, Z. Xuan, F. Du and Y. Zhong, *RSC Adv.*, 2016, **6**, 16730–16735.
20 Graphene Supermarket, https://graphene-supermarket.com/MoS2-Pristine-Flakes-in-Solution.html, accessed 24/11/2016.
21 S. J. Rowley-Neale, D. A. C. Brownson, J. M. Fearn, G. C. Smith, X. Ji and C. E. Banks, *Nanoscale*, 2016, **8**, 14767–14777.
22 S. Zhang, B. V. R. Chowdari, Z. Wen, J. Jin and J. Yang, *ACS Nano*, 2015, **9**, 12464–12472.
23 Sigma-Aldrich, http://www.sigmaaldrich.com/catalog/product/aldrich/804169?lang=en&region=GB, accessed 05/12/2016.

24 R. Kurapati, C. Backes, C. Ménard-Moyon, J. N. Coleman and A. Bianco, *Angew. Chem., Int. Ed.*, 2016, **55**, 5506–5511.
25 J. N. Coleman, M. Lotya, A. O'Neill, S. D. Bergin, P. J. King, U. Khan, K. Young, A. Gaucher, S. De, R. J. Smith, I. V. Shvets, S. K. Arora, G. Stanton, H.-Y. Kim, K. Lee, G. T. Kim, G. S. Duesberg, T. Hallam, J. J. Boland, J. J. Wang, J. F. Donegan, J. C. Grunlan, G. Moriarty, A. Shmeliov, R. J. Nicholls, J. M. Perkins, E. M. Grieveson, K. Theuwissen, D. W. McComb, P. D. Nellist and V. Nicolosi, *Science*, 2011, **331**, 568–571.
26 C. Backes, R. J. Smith, N. McEvoy, N. C. Berner, D. McCloskey, H. C. Nerl, A. O'Neill, P. J. King, T. Higgins, D. Hanlon, N. Scheuschner, J. Maultzsch, L. Houben, G. S. Duesberg, J. F. Donegan, V. Nicolosi and J. N. Coleman, *Nat. Commun.*, 2014, **5**, 4576.
27 L. Yadgarov, C. L. Choi, A. Sedova, A. Cohen, R. Rosentsveig, O. Bar-Elli, D. Oron, H. Dai and R. Tenne, *ACS Nano*, 2014, **8**, 3575–3583.
28 A. B. Laursen, A. S. Varela, F. Dionigi, H. Fanchiu, C. Miller, O. L. Trinhammer, J. Rossmeisl and S. Dahl, *J. Chem. Educ.*, 2012, **89**, 1595–1599.
29 D. Marin, F. Medicuti and C. Teijeiro, *J. Chem. Educ.*, 1994, **71**, A277.
30 N. A. Choudry, D. K. Kampouris, R. O. Kadara and C. E. Banks, *Electrochem. Commun.*, 2010, **12**, 6–9.
31 L. R. Cumba, J. P. Smith, D. A. C. Brownson, J. Iniesta, J. P. Metters, D. R. D. Carmo and C. E. Banks, *Analyst*, 2015, **140**, 1543–1550.
32 C. W. Foster, J. Pillay, J. P. Metters and C. E. Banks, *Sensors*, 2014, **14**, 21905–21922.
33 C. W. Foster, J. P. Metters and C. E. Banks, *Electroanalysis*, 2013, **25**, 2275–2282.
34 J. P. Metters, M. Gomez-Mingot, J. Iniesta, R. O. Kadara and C. E. Banks, *Sens. Actuators, B*, 2013, **177**, 1043–1052.